

Im aginary cubic oscillator  
and its square-well approxi m ation in  
p representation

M iloslav Znoj il<sup>1</sup>

y U stav jademe fyziky AV CR, 250 68 Rez, C zech Republic

A bstract

Schrodinger equation with the im aginary, P T sym m etric potential  $V(x) = ix^3$  is studied and discussed in m om entum representation, via a solvable square-well approximation of its kinetic term .

PACS 03.65.G e

---

<sup>1</sup>e-mail: znoj il@ ujf.cas.cz

# 1 Introduction

One-dimensional harmonic oscillator  $H^{(H.O.)} = p^2 + x^2$  is exactly solvable and appears in virtually any textbook on quantum mechanics. In the recently proposed PT symmetric quantum mechanics of Bender et al [1] a similar guiding role is played by the non-Hermitian cubic Hamiltonian  $H^{(C.O.)} = p^2 + ix^3$ . A straightforward numerical and semi-classical analysis of its Schrodinger equation

$$H^{(C.O.)} \psi_n = E_n^{(C.O.)} \psi_n; \quad n = 0, 1, \dots \quad (1)$$

supports the highly plausible conjecture that the spectrum of energies is real, discrete and bounded below [2]. The conjectured absence of its imaginary components is also indicated by the Hilbert-Schmidt analysis [3] and by the perturbation calculations in both the weak-coupling regime [4] and its strong-coupling, purely numerically generated rearrangements [5]. Also the numerical analytic continuation [6] and the so called exact semiclassical analysis [7] reveal numerous parallels to the Hermitian models.

Definitely, the problem deserves a deeper study. In what follows we shall modify the traditional perspective and work in the momentum representation. It gives the momentum as a mere number,  $p \in \mathbb{R}$ , and represents the coordinate  $x$  by the operator  $\hat{x} = i\partial_p$ . Equation (1) acquires a new form containing the purely real differential Schrodinger operator  $H^{(C.O.)} = E$  of the third order. This gives an unusual formulation of our bound-state problem,

$$\left( \frac{d^3}{dp^3} + p^2 \right) \psi(p) = E \psi(p); \quad \psi \in L_2(\mathbb{R}):$$

The quadratic  $p$  dependence of the kinetic term  $T(p) = p^2$  does not seem to make the equation any easier to solve. Here, we shall modify the kinetic term and offer the comprehensive analysis of the resulting square-well-type approximate form of the imaginary cubic oscillator.

## 2 Local solutions in a solvable simplification

In a way proposed by Prüfer [8] many wave functions can be visualized as certain "deformations"  $\psi(x) = c_1 \sin[k(x)] + c_2 \cos[k(x)]$  of solutions which correspond to a locally constant potential in the standard quantum mechanics. Such a type of an ansatz finds immediate applications in numerical computations [9] and leads to an easy interpretation [10] of the traditional Sturm-Liouville oscillation theorems [11]. Similar idea will also be used here as our main methodical guide.

### 2.1 Square-well approximation of the kinetic term

Let us replace the kinetic energy operator  $T(p) = p^2$  by the most elementary square well of a finite depth  $Z > 0$ ,

$$T(p) = \begin{cases} Z; & p^2 \in (-1; 1); \\ 0; & p^2 \in (-1; 1); \\ Z; & p^2 \in (1; 1): \end{cases}$$

In the bounded range of energies  $E < Z$  this enables us to split our toy model in the two separate differential equations,

$$\begin{aligned} \frac{d^3}{dp^3} \psi + 8^{-3} \psi &= 0; & p^2 \in (-1; 1); \\ \frac{d^3}{dp^3} \psi + 8^{-3} \psi &= 0; & p^2 \in (1; 1): \end{aligned}$$

The two auxiliary parameters  $\kappa = \kappa(E) > 0$  and  $\tilde{\kappa} = \tilde{\kappa}(E) > 0$  are defined in such a way that  $Z = E + 8^{-3} > E = 8^{-3}$ , and appear in the three independent (exponential) solutions of our equations. Their general superpositions are complex but may also be given the real, trigonometric form. In this way, near the origin we shall write

$$\psi_0(p) = d e^{2\kappa p} + f e^{-\kappa p} \cos(\tilde{\kappa} p + \phi); \quad p^2 \in (-1; 1); \quad \tilde{\kappa} = \sqrt{p^2 - 1}$$

where the symbols  $d$ ,  $f$  and  $\tilde{\epsilon}$  stand for the three undetermined constant parameters. In the right and left asymptotic regions we obtain the similar formulae. After we omit their unphysical and normalization-violating, exponentially growing components, we get the one-parametric family to the right,

$$\psi_+(p) = g e^{-2ip}; \quad p \geq (1; 1):$$

Its two-parametric left-barrier counterpart reads as follows,

$$\psi(p) = c e^{ip} \cos(\tilde{\epsilon} p + \alpha); \quad p \geq (-1; -1); \quad \tilde{\epsilon} = \frac{p}{3}:$$

At the right discontinuity  $p = 1$  we have to guarantee the continuity of  $\psi(p)$ ,  $\psi_p(p)$  and  $\psi_p^2(p)$ . This is equivalent to the three matching conditions

$$\begin{aligned} d e^2 + f e^{-\cos(\tilde{\epsilon} + \alpha)} &= g e^{-2}; \\ 2 d e^2 - f e^{-[\cos(\tilde{\epsilon} + \alpha) + \frac{p}{3} \sin(\tilde{\epsilon} + \alpha)]} &= -2 g e^{-2}; \\ 4^{-2} d e^2 - 2^{-2} f e^{-[\cos(\tilde{\epsilon} + \alpha) + \frac{p}{3} \sin(\tilde{\epsilon} + \alpha)]} &= 4^{-2} g e^{-2}; \end{aligned} \quad (2)$$

The weighted sum of these equations re-scales and interrelates the unknown coefficients  $d$  and  $g$  in terms of a new energy parameter  $t = t(E) = \tilde{\epsilon}(E) = \tilde{\epsilon}(E) > 0$  or rather  $R = R(E) = (1 - t + t^2)^{-1/2} > 0$ ,

$$d e^2 - D(E) = \frac{G(E)}{3 R^2(E)}; \quad G(E) = g e^{-2}:$$

After we eliminate  $G$  from the last two equations (2) which are linear in  $d$  and  $f$  we obtain the elementary formula which defines the shift  $\alpha = \alpha(E)$ ,

$$\tan(\tilde{\epsilon} + \alpha) = \frac{\frac{p}{3}}{2 - t - 1};$$

The trigonometric factors become fixed up to their common sign  $\mu = \pm 1$ ,

$$\cos(\tilde{\epsilon} + \alpha) = \mu [1 - t(E) = 2] R(E); \quad \sin(\tilde{\epsilon} + \alpha) = \frac{\frac{p}{3}}{2} \mu t(E) R(E):$$

The same sign also enters our last decoupled definition

$$f e^{-\alpha} = F(E) = \frac{2[t(E) + 1] G(E)}{3 \mu R(E)}:$$

Thus, up to an overall normalization (say,  $g = 1$ ), all the free parameters in our wave functions matched at  $p = 1$  become specified as functions of the energy.

At the second discontinuity  $p = -1$  we have to satisfy the other three matching conditions. In terms of the abbreviations

$$\begin{aligned} L_1 &= d e^{-2} + f e^{\cos(\tilde{\eta} + \eta)}; \\ L_2 &= 2 d e^{-2} - f e^{\left[\cos(\tilde{\eta} + \eta) + \frac{p}{\sqrt{3}} \sin(\tilde{\eta} + \eta)\right]}; \\ L_3 &= 4^{-2} d e^{-2} - 2^{-2} f e^{\left[\cos(\tilde{\eta} + \eta) + \frac{p}{\sqrt{3}} \sin(\tilde{\eta} + \eta)\right]} \end{aligned}$$

they read

$$\begin{aligned} L_1(\eta; d; f; p) &= c e^{\cos(\tilde{\eta} + \eta)}; \\ L_2(\eta; d; f; p) &= -c e^{\left[\cos(\tilde{\eta} + \eta) + \frac{p}{\sqrt{3}} \sin(\tilde{\eta} + \eta)\right]}; \\ L_3(\eta; d; f; p) &= -2^{-2} c e^{\left[\cos(\tilde{\eta} + \eta) + \frac{p}{\sqrt{3}} \sin(\tilde{\eta} + \eta)\right]}. \end{aligned}$$

In the same manner as above they determine the values of  $c = c(E)$  and  $\eta = \eta(E)$ .

Moreover, their properly weighted sum gives the equation

$$\frac{p}{\sqrt{3}} F(E) \sin(\tilde{\eta} + \eta) + (2t - 1) F(E) \cos(\tilde{\eta} + \eta) + 2 \frac{1 - t + t^2}{t + 1} D(E) e^{-6} = 0$$

or, after a slight rearrangement, the amazingly transparent relation

$$(1 - 4t + t^2) \cos\left(2\frac{p}{\sqrt{3}}\right) + \frac{p}{\sqrt{3}} (1 - t^2) \sin\left(2\frac{p}{\sqrt{3}}\right) = \frac{1 - t + t^2}{1 + t} e^{-3} : \quad (3)$$

It should be read as our desired *implicit* definition of the physical energies  $E$ .

## 2.2 $Z$ dependence of the toy spectrum

It is quite instructive to search for the physical energies numerically. Starting from the very-shallow-well extreme in eq. (3) we find the two clearly distinguished energy roots. The qualitative features of the graph remain unchanged in a broad interval of the "inverse strengths"  $1=Z$ . Its shape is sampled in Figure 1 at  $Z = 10^{-3}$ . We have tested that even the approximate height  $\approx 5$  of its left plateau stays virtually

unchanged in between  $Z = 10^{-5}$  and  $Z = 10^{-3}$ . Within the same interval of the shallowest wells the left zero grows from the value 0.00280 till 0.0241. Beyond the broad, downwards-oriented peak one finds the second, right zero moving from the value 0.01047 (found very close to the instantaneous threshold 0.01077) up the value 0.1056 (not very far from its threshold 0.1077, either) within the same interval of  $1=Z$ .

A new feature emerges around  $Z = 10^{-1}$  (with the left zero at 0.0445 and with the right zero 0.222 still quite close to the threshold 0.232) and  $Z = 1$  (with the left zero at 0.072 and with the right zero 0.446, not that close already to the threshold  $1=2$ ) in the left half of the picture. The plateau develops a local, safely negative maximum.

In the subsequent domain of  $Z > 1$  we have to switch our attention back to the right half of our graph. Immediately before the coupling reaches the integer value  $Z = 5$ , the end of the curve returns to the negative half-plane near the maximal (i.e., threshold) energy. This means that there emerges the third energy level there. The total number of bound states grows to  $N = 3$  (cf. the leftmost items in our Table 1).

Beyond  $Z = 5$ , our attention has to return quickly to the left half of the picture where the very slow growth of the local maximum creates a new quality at last. The top of the local bump touches and crosses the horizontal axis at  $Z = 5.3003$  and  $E = 0.6244$ . At  $Z = 5.3005$  a new doublet of energies is formed in a way illustrated in Figure 2. The number of levels jumps to  $N = 5$ .

A smooth deformation of the graph takes place when the value of  $Z$  grows on. During this evolution we discover that our (originally broad), downward-oriented peak shrinks quite quickly and moves comparatively slowly to the right. It gets close to the rightmost and, to its bad luck, slightly more slowly moving zero number five. The magnified picture of the resulting "collision" is displayed here in Figure 3. At  $Z = 35$  it shows that in the threshold region of the energies,

the wavy motion of the threshold end of our graph still did not manage to reach the zero axis;

the downwards-oriented peak has already left the positive part (and moved to the negative part) of the curve in question.

As a consequence, the number of levels drops, quite unexpectedly, down to 3 again (cf. Table 1).

In the vicinity of  $Z = 40$  the new, rightmost energy root emerges at last. Up to  $Z = 100$  and beyond, the number of levels stays equal to 4. Then it increases to 5, due to the emergence of the next threshold zero. Only after that, the slowly moving downward peak reaches the domain of the fourth zero. At almost exactly  $Z = 190$  its left (and temporarily negative) local maximum reaches the zero value again (cf. Figure 4). At this moment the number of states jumps up by two to seven. The magnified graphical proof is offered by Figure 5 at  $Z = 200$ . The latter Figure illustrates nicely the rapid shrinking of our peak with  $Z$ . The numerical detection of its position becomes more and more difficult. Although this position plays a crucial role in the practical determination of the number of levels at a given  $Z$ , we must be very careful in distinguishing the subgraph of Figure 5 (with three zeros) from a simple straight line with the single zero.

The pattern is deceitful and the standard software which searches for roots has to be used with a due care. Vice versa, the above analysis enables us to take into account all the specific features of the  $Z$  dependence of the graph in eq. (3). We get a regular pattern summarized in Table 1 and exhibiting a certain regularity of the  $Z$  dependence of the number of levels  $N = N(Z)$ .

### 3 Discussion

### 3.1 Energies in the square-well approximation

The main "physical" consequence of the presence of the above-mentioned narrow peak is an unusual irregularity observed in the emergence of the new levels in the deeper wells. We may conclude that this irregularity is not an artifact of the computation method. The energy formula (3) for our square-well toy model is exact and the seemingly unpredictable emergence of its roots just reflects the fact that our Schrodinger equation is of the third order. In particular, there exists no symmetry/antisymmetry with respect to the parity  $p \rightarrow -p$  etc.

Methodical consequences of our analysis are a bit discouraging. Firstly, the very symbolic-manipulation derivation of our present formulae proved unexpectedly complicated even in comparison with the multiple standard square wells in textbooks. That's why we did not move to any further piece-wise constant approximations of  $T(p)$ .

Secondly, even our use of the most elementary solvable example revealed quite clearly a very real danger of the possible loss of certain levels. For an illustration let us imagine that our numerical study would have been started in the deep-well domain, i.e., at the large  $Z$ . It is quite easy to generate the graphs of eq. (3) there. In the standard and routine finite-precision computer arithmetics one discovers that the results are very smooth and look virtually the same, say, in the interval of  $Z \in (1000; 1200)$ .

Let us pick up, for definiteness, the larger sample  $Z = 1200$ . We get a picture (cf. our last Figure 6) which is regular and, deceptively, indicates that  $N(1200) = 7$ . Unfortunately, the correct answer (appearing also at the right end of our Table 1) is  $N(1200) = 10$ . Its derivation requires the use of a significantly enhanced precision. Otherwise, whenever we use just the standard 14 digits and Figure 6, we would have missed as much as three (i.e., ca 30 % of all) energy levels.

In the light of our preceding considerations, an easy explanation of the latter



numerical paradox lies in the presence of the narrow peak. A priori, it is hardly predictable of course. It is necessary to spot it by brute force. One finds that at  $Z = 1000$ , this anomalous peak still lives safely below the sixth energy level. The related number of levels is reliably confirmed as equal to seven, indeed.

In between  $Z = 1000$  and  $Z = 1200$ , it is necessary to work in an enhanced precision arithmetics. One finds that the upper, threshold end of the curve crosses the horizontal axis only slightly above  $Z = 1100$ . Due to the very steep slope of the curve in this region, this crossing is not visible even at  $z = 1200$  in Figure 6.

One also has to trace the narrow peak carefully. It overtakes the sixth energy level at  $Z \approx 1190$  (and  $E = 4217$ ), in an arrangement resembling our Figure 4 above. Thus, one concludes, finally, that the new, almost degenerate pair of the energy levels emerges immediately beyond this point.

### 3.2 Wave functions and their zeros

A marginal merit of our use of the square-well-shaped  $T(p)$  lies in the availability of the explicit wave functions. For the lack of space we have to omit all the illustrative pictures and mention just a few of their most characteristic features.

In the first step we can notice that in the rightmost interval of the absence of any nodal zero in the wave function is in fact very similar to the usual Sturm-Liouvillean behaviour. Less expectedly, at the exact energy value one encounters an infinity of the nodal zeros in the leftmost subinterval of  $p \in (-1; 1)$ . In this domain we are fortunate in studying the exactly solvable case. The very presence of this infinite \textit{left} set of nodal zeros is extremely sensitive to the numerical level of precision we use. Indeed, the errors are proportional to the unphysical  $(\text{unphys:}) (p) \approx \exp(-2p)$  which is growing rapidly at  $p \rightarrow -1$ .

We may also note that after the smallest deviation of the energy  $E$  from its absolutely precise bound-state value even the non-numerical and absolutely precise wave

functions will be dominated by the growing asymptotics  $(\text{unphys.}) (p) \sim \exp(-2p)$  near the left infinity of course. After all, the change of sign of these asymptotics remains to be a reliable source of information about the fact that the energy just crossed its physical value. In practice, this observation could survive in the appropriate modifications of the "shooting" numerical algorithms [12] or in the rigorously proven versions of the so called method of Hill determinants [13]).

## 4 Outlook

We may summarize that in the standard momentum representation, we represented our Hamiltonian with the imaginary cubic interaction by the real differential expression. On a suitable Hilbert space this specifies the Hamiltonian operator with the numerical range (and, hence, spectrum) which is, obviously, real. This complements the extensive discussion of this topic in the recent literature (cf., e.g., [3] for its updated list).

We have touched here several immediate constructive consequences of the latter important observation. Being interested in the detailed structure of the energy spectrum first of all, we arrived at a consistent picture of some of its less standard features by using the suitable approximation of the kinetic term  $T(p)$ .

Our main observation is the regularity of the  $Z$ -dependence of the number  $N(Z)$  of the bound states (cf. Table 1). This indicates that one cannot rely upon any type of a simply modified Sturm-Liouvillean theory at present [14]. A slightly better chance of a possible future deduction of some simple oscillation-type theorems or rules seems only to exist within the middle interval of  $p^2 \in (-1; 1)$ . There, for a continuously growing energy parameter  $E$ , a steady right-ward movement of the nodal zeros competes with the exponential terms which are slowly varying. One can expect a further progress achieved by the further intensive study of the similar P T symmetric examples [15].

Our numerical experiments also inspire a number of the further open questions. Some of them emerge in the purely numerical context. In particular, a better understanding of the behaviour of the nodal zeros in the wave functions could help us to formulate an appropriate generalization of the Prüfer-type algorithms. One would like to find some rules replacing the standard oscillation theorems. Especially in the vicinity of the correct physical energies they could really lead, say, to some reliable and robust "right-to-left shooting" numerical recipe etc.

Several qualitative aspects of the problem became clarified even within our rough piecewise constant approximation of  $T(p)$ . We saw how the behaviour of the wave function asymptotics differs in the left and right infinity. In the vicinity of the origin  $p = 0$  the emergence and motion of the nodal zeros was interpreted in a graphical manner explaining some features of the  $N(Z)$  dependence. The loss of its monotonicity was confirmed by our solvable model.

The use of the momentum representation proved able to throw a new light on the counterintuitive bound states in  $PT$  symmetric quantum mechanics. The emergence/disappearance of our quasi-degenerate doublets should be emphasized as, perhaps, analogous to the unavoided level crossings in harmonic oscillators [16] and/or to the anomalous doubling of levels in the models of Natanzon type [17]. Perhaps, all the similar irregularities in the spectra should be attributed to some common peculiar combination of the analyticity and non-Hermiticity in all these unusual  $PT$  symmetric systems.

## Acknowledgement

Partially supported by the GA AS CR grant N r. A 104 8004.

## References

- [1] Bender C M , Boettcher S and Meisinger P N 1999 J. Math. Phys. 40 2201
- [2] Bessis D 1992 private communication;  
 Bender C M and Boettcher S 1998 Phys. Rev. Lett. 24 5243
- [3] Mezincoescu G A 2000 J. Phys. A : Math. Gen. 33 4911;  
 Bender C M 2001, a comment on previous paper, to appear
- [4] Caliceti E, Gra S and Maioli M 1980 Commun. Math. Phys. 75 51;  
 Bender C M and Weniger E J 2000 arXiv math-ph/0010007, submitted to J. Math. Phys.
- [5] Fernandez F M , Guardiola R , Ros J and Znojil M 1998 J. Phys. A : Math. Gen. 31 10105
- [6] Alvarez G 1995 J. Phys. A : Math. Gen. 27 4589;
- [7] Delabaere F and Pham F 1998 Phys. Lett. A 250 25;  
 Delabaere F and Trinh D T 2000 J. Phys. A : Math. Gen. 33 8771
- [8] Prufer H 1926 Math. Ann. 95 499
- [9] Uehla I, Havlcek M . and Horejs J 1981 Phys. Lett. A 82 64
- [10] Flugge S 1971 Practical quantum mechanics I (Berlin: Springer), p. 153
- [11] Ince E L 1956 Ordinary differential equations (New York: Dover), p. 223
- [12] Killingbeck J P, Gordon N A and Witwitt M R M 1995 Phys. Lett. A 206 279;  
 Znojil M 1997 Phys. Lett. A 230 283

- [13] Hautot A 1986 Phys. Rev. D 33 437;  
Znojil M 1992 J. Math. Phys. 33 213
- [14] Hille E 1969 Lectures on Ordinary Differential Equations (Reading: Addison-Wesley)
- [15] Bender C M , Boettcher S and Savage Van M 2000 J. Math. Phys. 41 6381
- [16] Znojil M 1999 Phys. Lett. A 259 220
- [17] Znojil M , Levai G , Roy P and Roychoudhury R 2001 Phys. Lett. A , submitted.

Tables

Table 1.  
Number of levels N and its changes with growing Z .

N	2	3	5	3	4	5	7	8	6	7	9	10
	1	2	2	1	1	2	1	2	1	2	1	

## Figure captions

Figure 1.

Graphical solution of equation (3) at  $Z = 1000$ .

Figure 2.

Local maximum giving the new doublet of roots at  $Z = 53005$ .

Figure 3.

The local maximum not giving the doublet of roots at  $Z = 35$ .

Figure 4.

Typical  $Z \ll 1$  graph of eq. (3) ( $Z = 190$ ).

Figure 5.

Quasi-degeneracy of the doublet of roots at  $Z = 200$ .

Figure 6.

Numerical invisibility of the narrow peak and of the new threshold root at  $Z = 1200$ .

Figure 1.

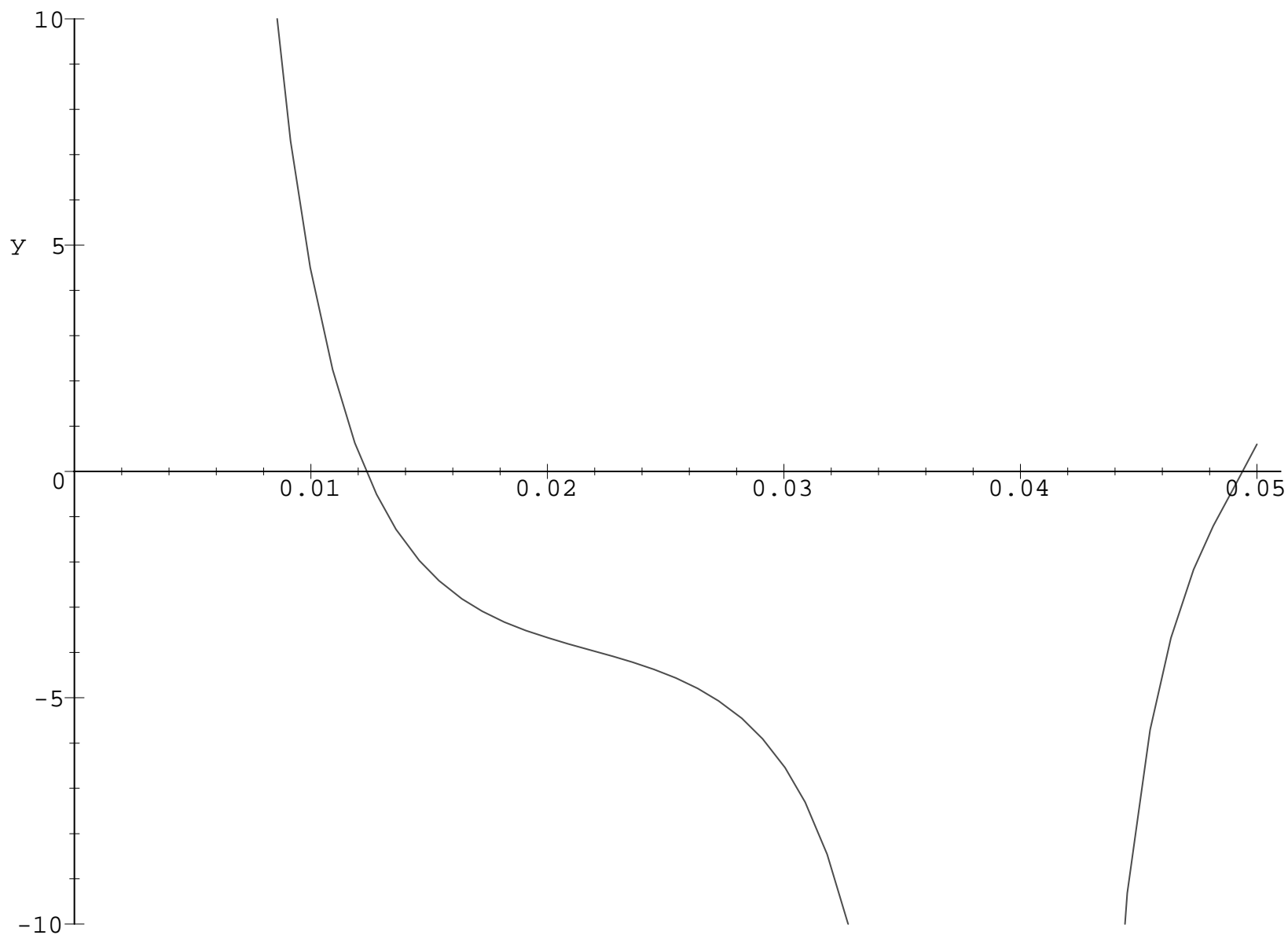




Figure 2.

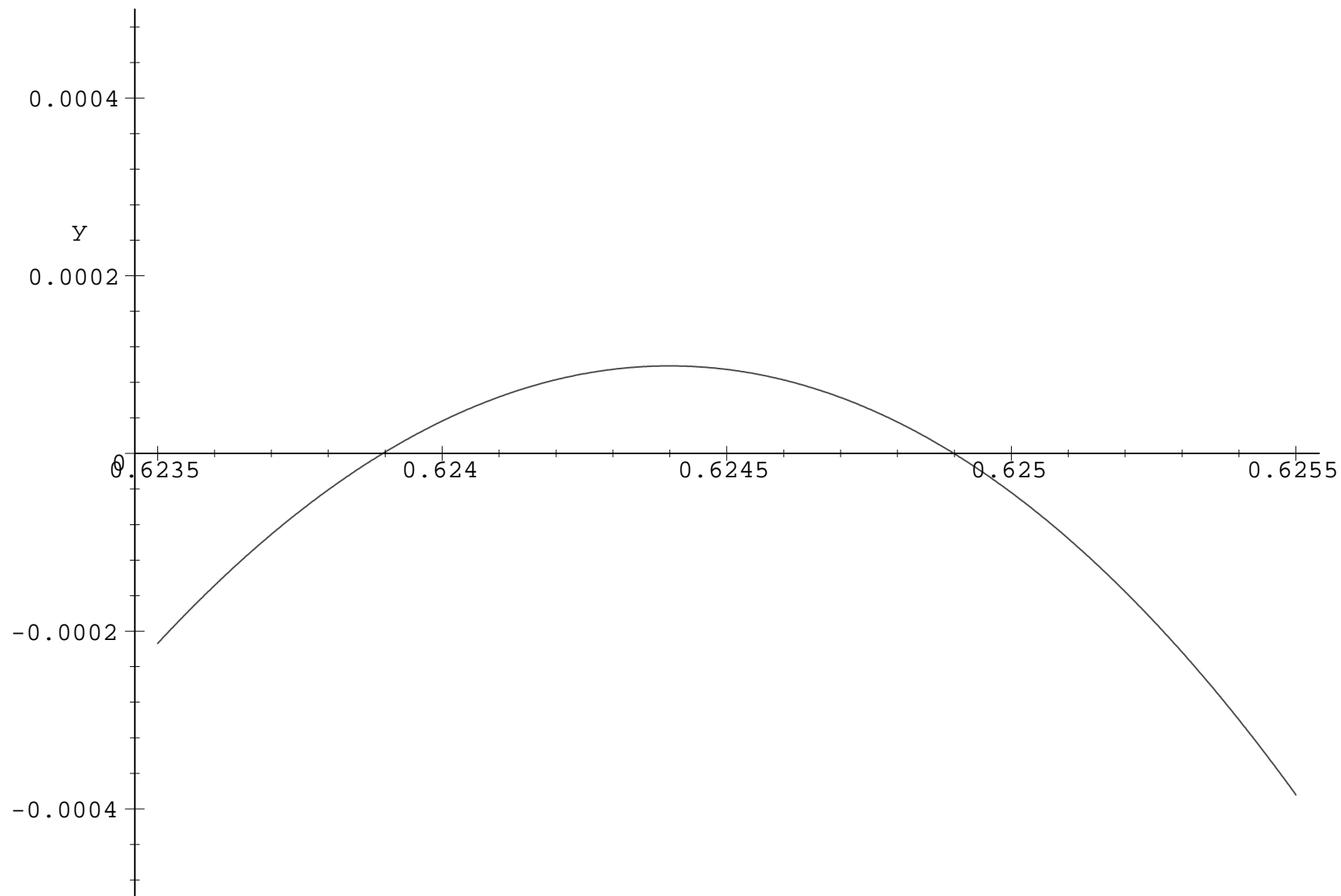


Figure 3.

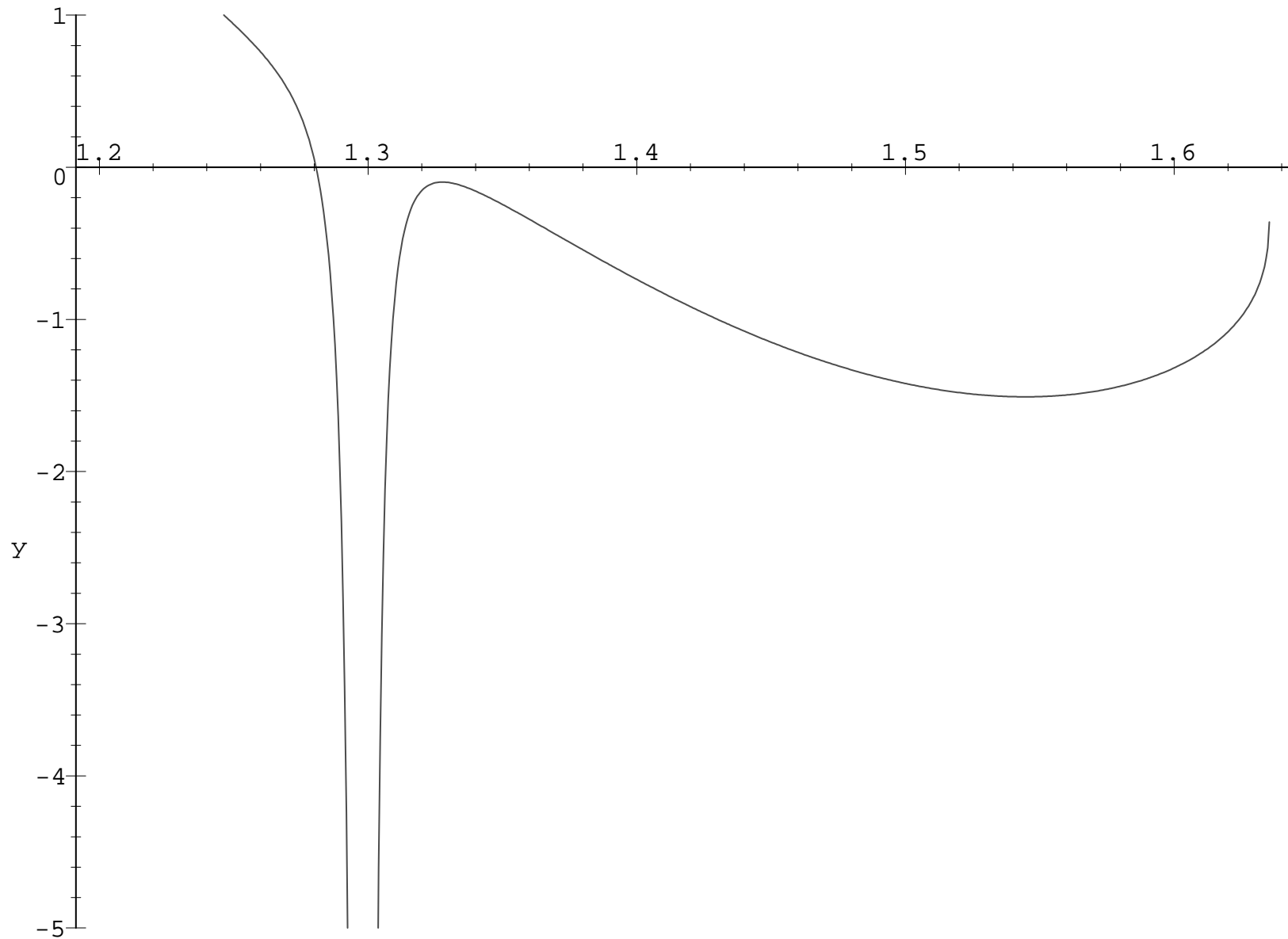


Figure 4.

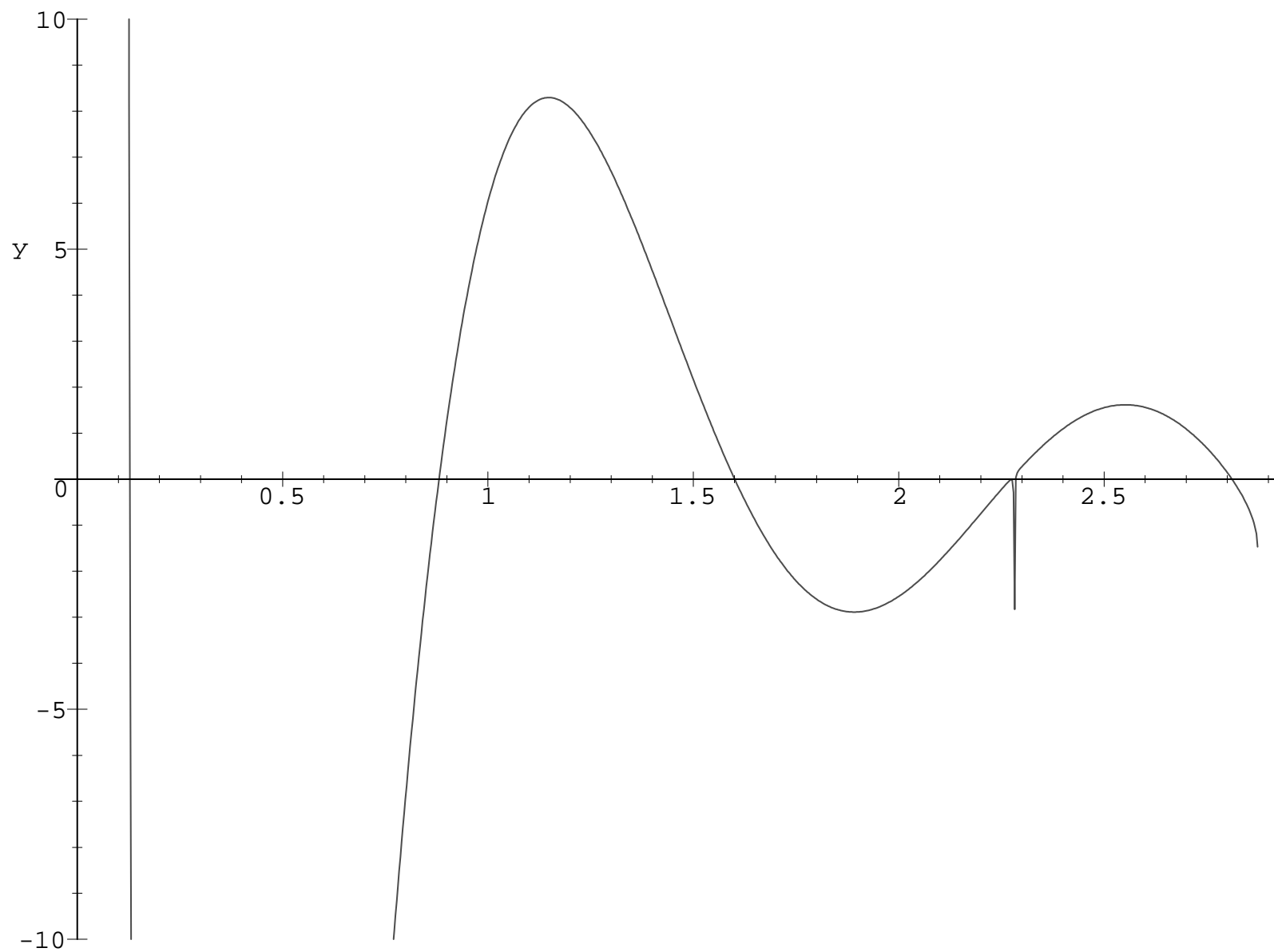


Figure 5.

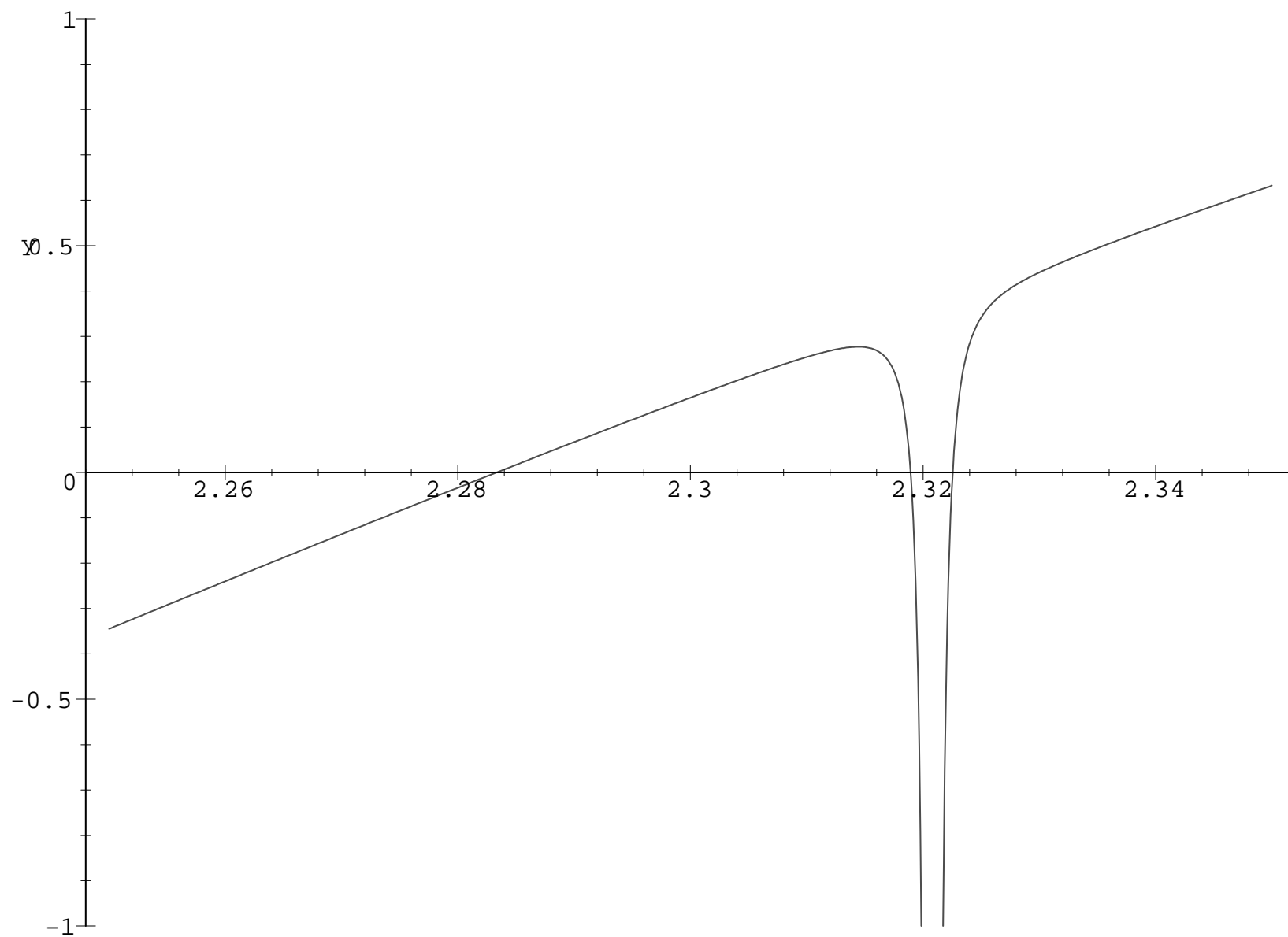
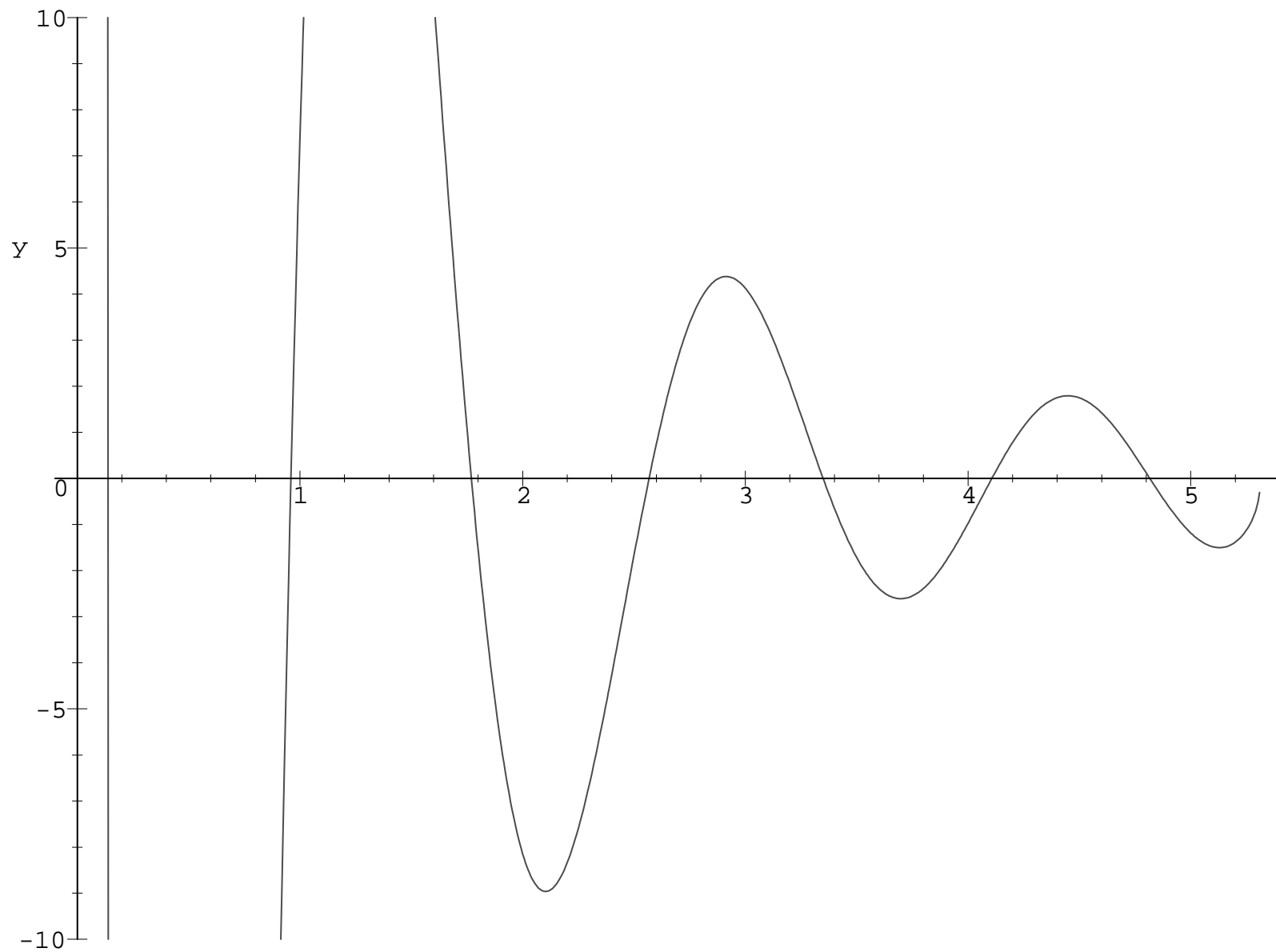


Figure 6.



# Imaginary cubic oscillator and its square-well approximation in $p$ -representation

Miloslav Znojil<sup>†1</sup>

<sup>†</sup> Ústav jaderné fyziky AV ČR, 250 68 Řež, Czech Republic

## Abstract

Schrödinger equation with the imaginary,  $\mathcal{PT}$  symmetric potential  $V(x) = i x^3$  is studied and discussed in momentum representation, via a solvable square-well approximation of its kinetic term.

PACS 03.65.Ge

---

<sup>1</sup>e-mail: znojil@ujf.cas.cz

# 1 Introduction

One-dimensional harmonic oscillator  $H^{(HO)} = p^2 + x^2$  is exactly solvable and appears in virtually any textbook on quantum mechanics. In the recently proposed  $\mathcal{PT}$  symmetric quantum mechanics of Bender et al [1] a similar guiding role is played by the non-Hermitian cubic Hamiltonian  $H^{(CO)} = p^2 + i x^3$ . A straightforward numerical and semi-classical analysis of its Schrödinger equation

$$H^{(CO)} |\psi_n\rangle = E_n^{(CO)} |\psi_n\rangle, \quad n = 0, 1, \dots \quad (1)$$

supports the highly plausible conjecture that the spectrum of energies is real, discrete and bounded below [2]. The conjectured absence of its imaginary components is also indicated by the Hilbert-Schmidt analysis [3] and by the perturbation calculations in both the weak-coupling regime [4] and its strong-coupling, purely numerically generated re-arrangements [5]. Also the numerical analytic continuation [6] and the so called exact semiclassical analysis [7] reveal numerous parallels to the Hermitian models.

Definitely, the problem deserves a deeper study. In what follows we shall modify the traditional perspective and work in the momentum representation. It gives the momentum as a mere number,  $p \in (-\infty, \infty)$ , and represents the coordinate  $x$  by the operator  $\hat{x} = i \partial_p$ . Equation (1) acquires a new form containing the *purely real* differential Schrödinger operator  $H^{(CO)} - E$  of the third order. This gives an unusual formulation of our bound-state problem,

$$\left[ \frac{d^3}{dp^3} + p^2 \right] \psi(p) = E \psi(p), \quad \psi(p) \in L_2(\mathbb{R}).$$

The quadratic  $p$ -dependence of the kinetic term  $T(p) = p^2$  does not seem to make the equation any easier to solve. Here, we shall modify the kinetic term and offer the comprehensive analysis of the resulting square-well-type approximate form of the imaginary cubic oscillator.

## 2 Local solutions in a solvable simplification

In a way proposed by Prüfer [8] many wave functions can be visualized as certain “deformations”  $\psi(x) \approx c_1 \sin[\varrho(x)] + c_2 \cos[\varrho(x)]$  of solutions which correspond to a locally constant potential in the standard quantum mechanics. Such a type of an ansatz finds immediate applications in numerical computations [9] and leads to an easy interpretation [10] of the traditional Sturm Liouvillean oscillation theorems [11]. Similar idea will also be used here as our main methodical guide.

### 2.1 Square-well approximation of the kinetic term

Let us replace the kinetic energy operator  $T(p) = p^2$  by the most elementary square well of a finite depth  $Z > 0$ ,

$$T(p) = \begin{cases} Z, & p \in (-\infty, -1), \\ 0, & p \in (-1, 1), \\ Z, & p \in (1, \infty). \end{cases}$$

In the bounded range of energies  $E < Z$  this enables us to split our toy model in the two separate differential equations,

$$\begin{aligned} \left[ \frac{d^3}{dp^3} - 8\alpha^3 \right] \psi(p) &= 0, & p \in (-1, 1), \\ \left[ \frac{d^3}{dp^3} + 8\beta^3 \right] \psi(p) &= 0, & p \in (-\infty, -1) \cup (1, \infty). \end{aligned}$$

The two auxiliary parameters  $\alpha = \alpha(E) > 0$  and  $\beta = \beta(E) > 0$  are defined in such a way that  $Z = E + 8\beta^3 > E = 8\alpha^3$ , and appear in the three independent (exponential) solutions of our equations. Their general superpositions are complex but may also be given the real, trigonometric form. In this way, near the origin we shall write

$$\psi_0(p) = d e^{2\alpha p} + f e^{-\alpha p} \cos(\tilde{\alpha} p + \theta), \quad p \in (-1, 1), \quad \tilde{\alpha} = \sqrt{3} \alpha$$



where the symbols  $d$ ,  $f$  and  $\theta$  stand for the three undetermined constant parameters. In the right and left asymptotic regions we obtain the similar formulae. After we omit their unphysical and normalization-violating, exponentially growing components, we get the one-parametric family to the right,

$$\psi_+(p) = g e^{-2\beta p}, \quad p \in (1, \infty).$$

Its two-parametric left-barrier counterpart reads as follows,

$$\psi_-(p) = c e^{\beta p} \cos(\tilde{\beta} p + \eta), \quad p \in (-\infty, -1), \quad \tilde{\beta} = \sqrt{3} \beta.$$

At the right discontinuity  $p = 1$  we have to guarantee the continuity of  $\psi(p)$ ,  $\partial_p \psi(p)$  and  $\partial_p^2 \psi(p)$ . This is equivalent to the three matching conditions

$$\begin{aligned} d e^{2\alpha} + f e^{-\alpha} \cos(\tilde{\alpha} + \theta) &= g e^{-2\beta}, \\ 2\alpha d e^{2\alpha} - \alpha f e^{-\alpha} [\cos(\tilde{\alpha} + \theta) + \sqrt{3} \sin(\tilde{\alpha} + \theta)] &= -2\beta g e^{-2\beta}, \\ 4\alpha^2 d e^{2\alpha} - 2\alpha^2 f e^{-\alpha} [\cos(\tilde{\alpha} + \theta) - \sqrt{3} \sin(\tilde{\alpha} + \theta)] &= 4\beta^2 g e^{-2\beta}. \end{aligned} \quad (2)$$

The weighted sum of these equations re-scales and interrelates the unknown coefficients  $d$  and  $g$  in terms of a new energy parameter  $t = t(E) = \beta(E)/\alpha(E) > 0$  or rather  $R = R(E) = (1 - t + t^2)^{-1/2} > 0$ ,

$$d e^{2\alpha} \equiv D(E) = \frac{G(E)}{3 R^2(E)}, \quad G(E) \equiv g e^{-2\beta}.$$

After we eliminate  $G$  from the last two equations (2) which are linear in  $d$  and  $f$  we obtain the elementary formula which defines the shift  $\theta = \theta(E)$ ,

$$\tan(\tilde{\alpha} + \theta) = \frac{\sqrt{3}}{2/t - 1}.$$

The trigonometric factors become fixed up to their common sign  $\varepsilon = \pm 1$ ,

$$\cos(\tilde{\alpha} + \theta) = \varepsilon [1 - t(E)/2] R(E), \quad \sin(\tilde{\alpha} + \theta) = \frac{\sqrt{3}}{2} \varepsilon t(E) R(E).$$

The same sign also enters our last decoupled definition

$$f e^{-\alpha} \equiv F(E) = \frac{2[t(E) + 1] G(E)}{3 \varepsilon R(E)}.$$

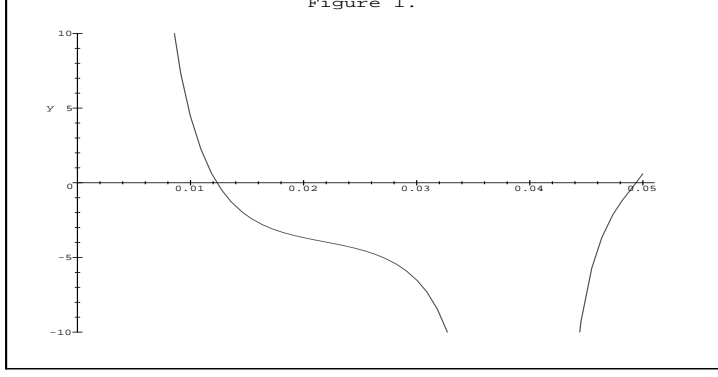


Figure 1: Graphical solution of equation (3) at  $Z = 1/1000$ .

Thus, up to an overall normalization (say,  $g = 1$ ), all the free parameters in our wave functions matched at  $p = 1$  become specified as functions of the energy.

At the second discontinuity  $p = -1$  we have to satisfy the other three matching conditions. In terms of the abbreviations

$$\begin{aligned} L_1 &= d e^{-2\alpha} + f e^{\alpha} \cos(-\tilde{\alpha} + \theta), \\ L_2 &= 2\alpha d e^{-2\alpha} - \alpha f e^{\alpha} [\cos(-\tilde{\alpha} + \theta) + \sqrt{3} \sin(-\tilde{\alpha} + \theta)], \\ L_3 &= 4\alpha^2 d e^{-2\alpha} - 2\alpha^2 f e^{\alpha} [\cos(-\tilde{\alpha} + \theta) - \sqrt{3} \sin(-\tilde{\alpha} + \theta)] \end{aligned}$$

they read

$$\begin{aligned} L_1(\alpha, d, f, \theta) &= c e^{-\beta} \cos(-\tilde{\beta} + \eta), \\ L_2(\alpha, d, f, \theta) &= \beta c e^{-\beta} [\cos(-\tilde{\beta} + \eta) - \sqrt{3} \sin(-\tilde{\beta} + \eta)], \\ L_3(\alpha, d, f, \theta) &= -2\beta^2 c e^{-\beta} [\cos(-\tilde{\beta} + \eta) + \sqrt{3} \sin(-\tilde{\beta} + \eta)]. \end{aligned}$$

In the same manner as above they determine the values of  $c = c(E)$  and  $\eta = \eta(E)$ .

Moreover, their properly weighted sum gives the equation

$$\sqrt{3} F(E) \sin(-\tilde{\alpha} + \theta) + (2t - 1) F(E) \cos(-\tilde{\alpha} + \theta) + 2 \frac{1 - t + t^2}{t + 1} D(E) e^{-6\alpha} = 0$$

or, after a slight re-arrangement, the amazingly transparent relation

$$(1 - 4t + t^2) \cos(2\sqrt{3}\alpha) + \sqrt{3}(1 - t^2) \sin(2\sqrt{3}\alpha) = \left( \frac{1 - t + t^2}{1 + t} e^{-3\alpha} \right)^2. \quad (3)$$

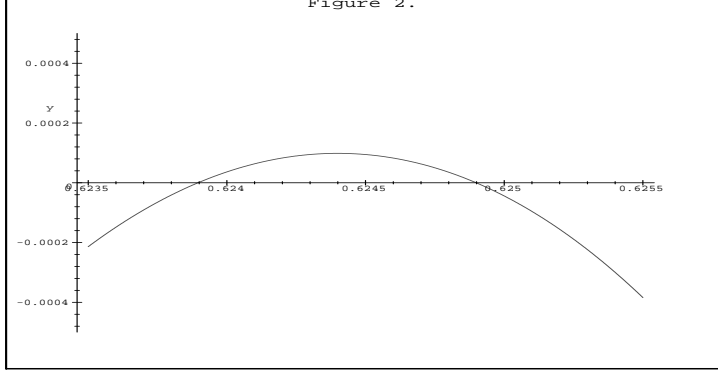


Figure 2: Local maximum giving the new doublet of roots at  $Z = 5.3005$ .

It should be read as our desired final implicit definition of the physical energies  $E$ .

## 2.2 $Z$ –dependence of the toy spectrum

It is quite instructive to search for the physical energies numerically. Starting from the very-shallow-well extreme in eq. (3) we find the two clearly distinguished energy roots. The qualitative features of the graph remain unchanged in a broad interval of the “inverse strengths”  $1/Z$ . Its shape is sampled in Figure 1 at  $Z = 10^{-3}$ .

We have tested that even the approximate height  $\approx -5$  of its left plateau stays virtually unchanged in between  $Z = 10^{-5}$  and  $Z = 10^{-3}$ . Within the same interval of the shallowest wells the left zero grows from the value 0.00280 till 0.0241. Beyond the broad, downwards-oriented peak one finds the second, right zero moving from the value 0.01047 (found very close to the instantaneous threshold 0.01077) up the value 0.1056 (not very far from its threshold 0.1077, either) within the same interval of  $1/Z$ .

A new feature emerges around  $Z = 10^{-1}$  (with the left zero at 0.0445 and with the right zero 0.222 still quite close to the threshold 0.232) and  $Z = 1$  (with the left zero at 0.072 and with the right zero 0.446, not that close already to the threshold

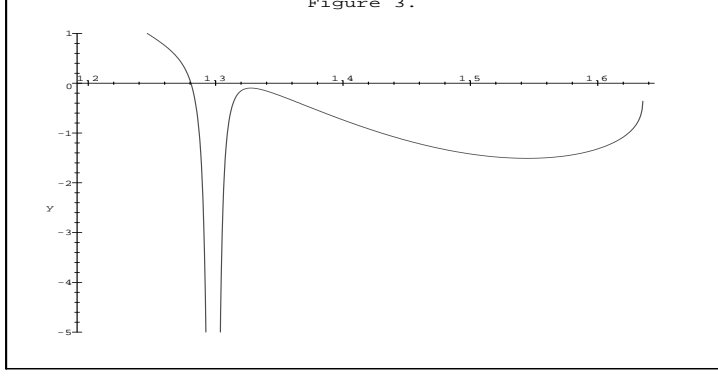


Figure 3: The local maximum not giving the doublet of roots at  $Z = 35$ .

1/2) in the left half of the picture. The plateau develops a local, safely negative maximum.

In the subsequent domain of  $Z > 1$  we have to switch our attention back to the right half of our graph. Immediately before the coupling reaches the integer value  $Z = 5$ , the end of the curve returns to the negative half-plane near the maximal (i.e., threshold) energy. This means that there emerges the third energy level there. The total number of bound states grows to  $N = 3$  (cf. the leftmost items in our Table 1).

Beyond  $Z = 5$ , our attention has to return quickly to the left half of the picture where the very slow growth of the local maximum creates a new quality at last. The top of the local bump touches and crosses the horizontal axis at  $Z \approx 5.3003$  and  $E \approx 0.6244$ . At  $Z = 5.3005$  a new doublet of energies is formed in a way illustrated in Figure 2. The number of levels jumps to  $N = 5$ .

A smooth deformation of the graph takes place when the value of  $Z$  grows on. During this evolution we discover that our (originally broad), downward-oriented peak shrinks quite quickly and moves comparatively slowly to the right. It gets close to the rightmost and, to its bad luck, slightly more slowly moving zero number five. The magnified picture of the resulting “collision” is displayed here in Figure 3. At

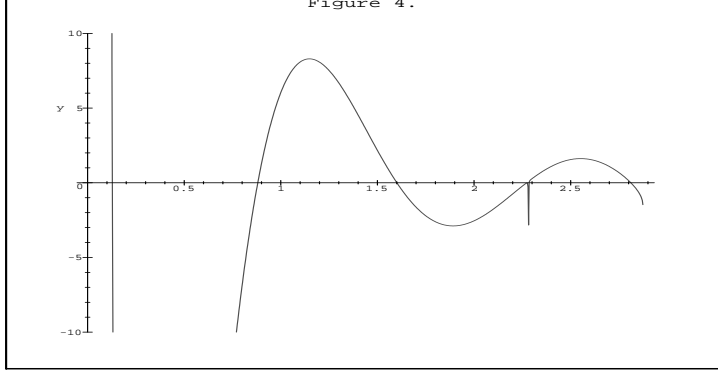


Figure 4: Typical  $Z \gg 1$  graph of eq. (3) ( $Z = 190$ ).

$Z = 35$  it shows that in the threshold region of the energies,

- the wavy motion of the threshold end of our graph still did not manage to reach the zero axis;
- the downwards-oriented peak has already left the positive part (and moved to the negative part) of the curve in question.

As a consequence, the number of levels drops, quite unexpectedly, down to 3 again (cf. Table 1).

In the vicinity of  $Z = 40$  the new, rightmost energy root emerges at last. Up to  $Z = 100$  and beyond, the number of levels stays equal to 4. Then it increases to 5, due to the emergence of the next threshold zero. Only after that, the slowly moving downward peak reaches the domain of the fourth zero. At almost exactly  $Z = 190$  its left (and temporarily negative) local maximum reaches the zero value again (cf. Figure 4).

At this moment the number of states jumps up by two to seven. The magnified graphical proof is offered by Figure 5 at  $Z = 200$ .

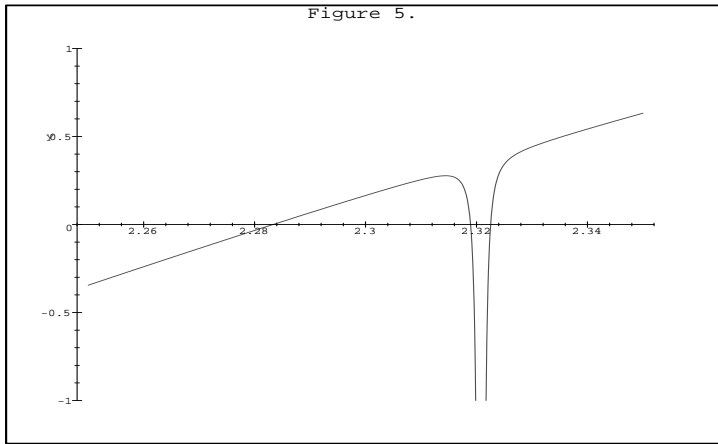


Figure 5: Quasi-degeneracy of the doublet of roots at  $Z = 200$ .

The latter Figure illustrates nicely the rapid shrinking of our peak with  $Z$ . The numerical detection of its position becomes more and more difficult. Although this position plays a crucial role in the practical determination of the number of levels at a given  $Z$ , we must be very careful in distinguishing the subgraph of Figure 5 (with three zeros) from a simple straight line with the single zero.

The pattern is deceitful and the standard software which searches for roots has to be used with a due care. *Vice versa*, the above analysis enables us to take into account all the specific features of the  $Z$ -dependence of the graph in eq. (3). We get a regular pattern summarized in Table 1 and exhibiting a certain regularity of the  $Z$ -dependence of the number of levels  $N = N(Z)$ .

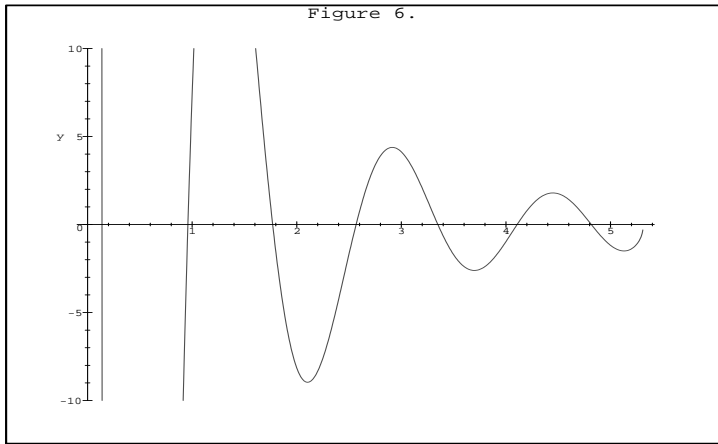


Figure 6: Numerical invisibility of the narrow peak and of the new threshold root at  $Z = 1200$ .

### 3 Discussion

#### 3.1 Energies in the square-well approximation

The main “physical” consequence of the presence of the above-mentioned narrow peak is an unusual irregularity observed in the emergence of the new levels in the deeper wells. We may conclude that this irregularity is not an artifact of the computation method. The energy formula (3) for our square-well toy model is exact and the seemingly unpredictable emergence of its roots just reflects the fact that our Schrödinger equation is of the third order. In particular, there exists no symmetry/antisymmetry with respect to the parity  $p \rightarrow -p$  etc.

Methodical consequences of our analysis are a bit discouraging. Firstly, the very symbolic-manipulation derivation of our present formulae proved unexpectedly complicated even in comparison with the multiple standard square wells in textbooks. That’s why we did not move to any further piece-wise constant approximations of  $T(p)$ .

Secondly, even our use of the most elementary solvable example revealed quite clearly a very real danger of the possible loss of certain levels. For an illustration let us imagine that our numerical study would have been started in the deep-well domain, i.e., at the large  $Z$ . It is quite easy to generate the graphs of eq. (3) there. In the standard and routine finite-precision computer arithmetics one discovers that the results are very smooth and look virtually the same, say, in the interval of  $Z \in (1000, 1200)$ .

Let us pick up, for definiteness, the larger sample  $Z = 1200$ . We get a picture (cf. Figure 6) which is regular and, deceptively, indicates that  $N(1200) = 7$ . Unfortunately, the correct answer (appearing also at the right end of our Table 1) is  $N(1200) = 10$ . Its derivation requires the use of a significantly enhanced precision. Otherwise, whenever we use just the standard 14 digits and Figure 6, we would have missed as much as three (i.e., cca 30 % of all) energy levels.

In the light of our preceding considerations, an easy explanation of the latter numerical paradox lies in the presence of the narrow peak. *A priori*, it is hardly predictable of course. It is necessary to spot it by brute force. One finds that at  $Z = 1000$ , this anomalous peak still lives safely below the sixth energy level. The related number of levels is reliably confirmed as equal to seven, indeed.

In between  $Z = 1000$  and  $Z = 1200$ , it is necessary to work in an enhanced precision arithmetics. One finds that the upper, threshold end of the curve crosses the horizontal axis only slightly above  $Z = 1100$ . Due to the very steep slope of the curve in this region, this crossing is not visible even at  $z = 1200$  in Figure 6.

One also has to trace the narrow peak carefully. It overtakes the sixth energy level at  $Z \approx 1190$  (and  $E = 4.217$ ), in an arrangement resembling our Figure 4 above. Thus, one concludes, finally, that the new, almost degenerate pair of the energy levels emerges immediately beyond this point.



### 3.2 Wave functions and their zeros

A marginal merit of our use of the square-well-shaped  $T(p)$  lies in the availability of the explicit wave functions. For the lack of space we have to omit all the illustrative pictures and mention just a few of their most characteristic features.

In the first step we can notice that in the rightmost interval of  $p$  the absence of any nodal zero in the wave function is in fact very similar to the usual Sturm Liouvillean behaviour. Less expectedly, at the exact energy value one encounters an infinity of the nodal zeros in the leftmost subinterval of  $p \in (-\infty, -1)$ . In this domain we are fortunate in studying the exactly solvable case. The very presence of this infinite “left” set of nodal zeros is extremely sensitive to the numerical level of precision we use. Indeed, the errors are proportional to the unphysical  $\psi^{(unphys.)}(p) \sim \exp(-2\beta p)$  which is growing rapidly at  $p \ll -1$ .

We may also note that after the smallest deviation of the energy  $E$  from its absolutely precise bound-state value even the non-numerical and absolutely precise wave functions will be dominated by the growing asymptotics  $\psi^{(unphys.)}(p) \sim \exp(-2\beta p)$  near the left infinity of course. After all, the change of sign of these asymptotics remains to be a reliable source of information about the fact that the energy just crossed its physical value. In practice, this observation could survive in the appropriate modifications of the “shooting” numerical algorithms [12] or in the rigorously proven versions of the so called method of Hill determinants [13]).

## 4 Outlook

We may summarize that in the standard momentum representation, we represented our Hamiltonian with the imaginary cubic interaction by the *real* differential expression. On a suitable Hilbert space this specifies the Hamiltonian operator with the numerical range (and, hence, spectrum) which is, obviously, real. This complements

the extensive discussion of this topic in the recent literature (cf., e.g., [3] for its updated list).

We have touched here several immediate *constructive* consequences of the latter important observation. Being interested in the detailed structure of the energy spectrum first of all, we arrived at a consistent picture of some of its less standard features by using the suitable approximation of the kinetic term  $T(p)$ .

Our main observation is the regularity of the  $Z$ –dependence of the number  $N(Z)$  of the bound states (cf. Table 1). This indicates that one cannot rely upon any type of a simply modified Sturm-Liouvillean theory at present [14]. A slightly better chance of a possible future deduction of some simple oscillation-type theorems or rules seems only to exist within the middle interval of  $p \in (-1, 1)$ . There, for a continuously growing energy parameter  $E$ , a steady right-ward movement of the nodal zeros competes with the exponential terms which are slowly varying. One can expect a further progress achieved by the further intensive study of the similar  $\mathcal{PT}$  symmetric examples [15].

Our numerical experiments also inspire a number of the further open questions. Some of them emerge in the purely numerical context. In particular, a better understanding of the behaviour of the nodal zeros in the wave functions could help us to formulate an appropriate generalization of the Prüfer-type algorithms. One would like to find some rules replacing the standard oscillation theorems. Especially in the vicinity of the correct physical energies they could really lead, say, to some reliable and robust “right-to-left shooting” numerical recipe etc.

Several qualitative aspects of the problem became clarified even within our rough piece-wise constant approximation of  $T(p)$ . We saw how the behaviour of the wave function asymptotics differs in the left and right infinity. In the vicinity of the origin  $p \approx 0$  the emergence and motion of the nodal zeros was interpreted in a graphical manner explaining some features of the  $N(Z)$  dependence. The loss of its monotonicity was confirmed by our solvable model.

The use of the momentum representation proved able to throw a new light on the counterintuitive bound states in  $\mathcal{PT}$  symmetric quantum mechanics. The emergence/disappearance of our quasi-degenerate doublets should be emphasized as, perhaps, analogous to the unavoided level crossings in harmonic oscillators [16] and/or to the anomalous doubling of levels in the models of Natanzon type [17]. Perhaps, all the similar irregularities in the spectra should be attributed to some common peculiar combination of the analyticity and non-Hermiticity in all these unusual  $\mathcal{PT}$  symmetric systems.

## Acknowledgement

Partially supported by the GA AS CR grant Nr. A 104 8004.

## Tables

Table 1.

**Number of levels  $N$  and its changes  $\Delta$  with growing  $Z$ .**

$N$	2	3	5	3	4	5	7	8	6	7	9	10
$\Delta$	1	2	-2	1	1	2	1	-2	1	2	1	

# References

- [1] Bender C M, Boettcher S and Meisinger P N 1999 J. Math. Phys. 40 2201
- [2] Bessis D 1992 private communication;  
Bender C M and Boettcher S 1998 Phys. Rev. Lett. 24 5243
- [3] Mezincescu G A 2000 J. Phys. A: Math. Gen. 33 4911;  
Bender C M 2001, a comment on previous paper, to appear
- [4] Caliceti E, Graffi S and Maioli M 1980 Commun. Math. Phys. 75 51;  
Bender C M and Weniger E J 2000 arXive math-ph/0010007, submitted to J. Math. Phys.
- [5] Fernández F M, Guardiola R, Ros J and Znojil M 1998 J. Phys. A: Math. Gen. 31 10105
- [6] Alvarez G 1995 J. Phys. A: Math. Gen. 27 4589;
- [7] Delabaere F and Pham F 1998 Phys. Lett. A 250 25;  
Delabaere F and Trinh D T 2000 J. Phys. A: Math. Gen. 33 8771
- [8] Prüfer H 1926 Math. Ann. 95 499
- [9] Úlehla I, Havlíček M. and Hořejší J 1981 Phys. Lett. A 82 64
- [10] Flügge S 1971 Practical quantum mechanics I (Berlin: Springer), p. 153
- [11] Ince E L 1956 Ordinary differential equations (New York: Dover), p. 223
- [12] Killingbeck J P, Gordon N A and Witwit M R M 1995 Phys. Lett. A 206 279;  
Znojil M 1997 Phys. Lett. A 230 283

- [13] Hautot A 1986 Phys. Rev. D 33 437;  
Znojil M 1992 J. Math. Phys. 33 213
- [14] Hille E 1969 Lectures on Ordinary Differential Equations (Reading: Addison-Wesley)
- [15] Bender C M, Boettcher S and Savage Van M 2000 J. Math. Phys. 41 6381
- [16] Znojil M 1999 Phys. Lett. A 259 220
- [17] Znojil M, Lévai G, Roy P and Roychoudhury R 2001 Phys. Lett. A, submitted.